# Measurement of Carbon on Cold-Rolled Steel: A Comparative Study Using Surface Analytical and Coulometric Methodologies

**James E. deVries,* Larry P. Haack, and Phillip L. Coduti†**

*Ford Motor Company, Mail Drop 3061 SRL, Dearborn, MI 48121*

Three cold-rolled steels manufactured under different mill-processing conditions were analyzed by X-ray photoelectron spectroscopy (XPS), secondary ion mass spectrometry (SIMS) and direct oxidation $CO_2$ coulometry (DOCC). XPS and SIMS depth profiling were also used to characterize the steels after successive DOCC oxidative treatments at 450 and 600 °C in order to assess what type of carbon is consumed and what analysis depth is probed at each stage of the DOCC measurement. XPS experiments involving *in situ* oxidative treatments revealed that, for each steel, all detectable surface carbon is removed at 450 °C. SIMS depth profile analyses determined that $Fe_2O_3$ layers formed during the 450 and 600 °C DOCC combustion processes were approximately 200 and 2000 nm thick, respectively, revealing that near surface inorganic carbon is also measured during the DOCC analysis. Nevertheless, it was concluded that the DOCC analysis at 450 °C measures mostly surface organic carbon, since the near surface carbon contribution is minor. The subsequent 600 °C DOCC measurement is comprised entirely of near surface inorganic carbon and is reflective of the process control conditions used to manufacture the steel.

## Introduction

The ability to manufacture and prepare surfaces free from carbon-containing contaminants is important both technically and economically to a number of industries. Measuring the amount of carbon present on sheet steel surfaces is a widely recognized way of assessing steel surface cleanliness (Coduti and Smith, 1979; Coduti, 1980; Hospadaruk et al., 1978; Wojtkowiak and Bender, 1979; Fisher et al., 1980; Iezzi and Leidheiser, 1981; Leroy et al., 1984). The majority of surface carbon analysis methods reported in the literature consist of heating metal samples in the presence of $O_2$, thereby converting the surface carbon to $CO_2$, and measuring the amount of $CO_2$ produced. Investigations have included the measurement of the $CO_2$ by manometric (Boggs and Pellissier, 1967), conductometric (Solet, 1950), and thermal conductivity (Lee and Lewis, 1970) methodologies. Wojtkowiak and Bender (1980) reported using a stream of nitrogen and a thermal evolution analyzer to sweep volatile organic species into a flame ionization detector.

Direct oxidation $CO_2$ coulometry (DOCC) was employed in this study. In this technique carbon on steel is combusted sequentially in two separate heating zones with $O_2$ to form $CO_2$, which is measured by coulometry. The first heating zone, set at 450 °C, is designed to react the surface organic carbon, while the second heating zone, set at 600 °C, combusts any remaining inorganic carbon.

The DOCC technique has been used in a number of diverse applications to obtain measurements of surface carbon on a variety of steel surfaces (Coduti, 1981, 1982). Analyses have also been expanded to the investigations of surface carbon on electrogalvanized steel, hot-dipped galvanized steel, galvannealed steel, stainless steel, aluminum, catalysts, silicon wafers, ceramics, and glasses (King, 1978). This method has been also incorporated as an in-plant statistical process control tool for monitoring surface cleanliness (Pumnea and Stadnick, 1988).

X-ray photoelectron spectroscopy (XPS) and secondary ion mass spectrometry (SIMS) techniques were used to explicitly define and quantify the surface carbon and oxide present on cold-rolled steel (CRS) before and after the various stages of the DOCC experiment. XPS analyses of the steels heated *in situ* were also undertaken to mimic the coulometric experiments. SIMS depth profiles were obtained on samples before and after each DOCC oxidation step to determine how the surface and near surface of the steels were modified by each treatment.

## Experimental Section

**Materials.** Three low-carbon (0.05-0.07 wt %) CRS samples, supplied by Inland Steel Company, East Chicago, IN, were selected from three steel coils having different mill-processing histories (i.e., tandem reduction, batch annealing, and temper rolling). Reference materials of iron carbide ($Fe_3C$, 99% pure) and gray cast iron (pig iron containing 4.0% carbon) were obtained from Alpha Products, Danvers, MA, and Inland Steel, respectively. These materials were used for XPS and SIMS iron carbide characterization and compared with data acquired on the three steel samples.

Prior to analysis, steel test panels measuring 10 × 30 cm were laboratory spray power washed (Coduti and Earl, 1980). This procedure simulates commercial alkaline-cleaning processes and removes any loosely bound oils and surface soils, with minimal disturbance to the tenaciously bound surface carbon. Test strips measuring 1 × 10 cm, with a 0.48 cm diameter hole at one end, were punched out of the spray power washed panels using a clean punch press. The test strips were then immediately analyzed by the DOCC technique. Companion steel samples for XPS and SIMS characterization were stored in a desiccator until analysis.

**Direct Oxidation $CO_2$ Coulometric Measurements.** The Model 5010 $CO_2$ coulometer used in this study was manufactured by Coulometrics, Inc., Wheat

* To whom correspondence should be addressed. E-mail address: jdevries@smail.srl.ford.com.

† Inland Steel Flat Products Company, Research Laboratories, 3001 E. Columbus Dr., East Chicago, IN 46312.

0888-5885/94/2633-2618$04.50/0 

**Table 1. Percent Carbon Recovery for Organic and Nonorganic Carbon-Containing Substances at 450 and 600 °C during DOCC Analysis[a]**

| substance | zone 1 at 450 °C | zone 2 at 600 °C |
|---|---|---|
| sucrose | >99% | <1% |
| dioctylsebacate | >99% | <1% |
| rust preventative oil | ≥97% | ≤3% |
| acrylic acid resin | >99% | <1% |
| $Fe_3C$ | ≤7% | >41%[b] |
| carbon black | ≤12% | ≥88% |
| graphite | ≤10% | >85%[b] |
| $CaCO_3$ | ≤2% | >37%[b] |

[a] 3 mg samples were placed in zone 1, first for a 5 min dwell time, and then moved to zone 2, in situ, for an additional 5 min. [b] $CO_2$ continued to evolve after the 5 min dwell time in zone 2.

**Table 2. DOCC Results for CRS Samples**

| CRS | carbon measurement (mg/m²) | | |
|---|---|---|---|
| | organic | nonorganic | total |
| sample 1 | 2.58 | 2.15 | 4.73 |
| sample 2 | 4.08 | 3.65 | 7.74 |
| sample 3 | 9.78 | 9.14 | 18.9 |

**Table 3. XPS Quantitative Results of the Alkaline Cleaned (Virgin Surfaces) CRS Samples**

| CRS | composition (at. %) | | | | | | | C/Fe ratio |
|---|---|---|---|---|---|---|---|---|
| | C | O | Fe | P | Ca | N | Mn | |
| sample 1 | 43.0 | 45.0 | 6.3 | 2.0 | 1.8 | 2.0 | 0.2 | 6.8 |
| sample 2 | 62.0 | 30.0 | 3.9 | 0.6 | 0.9 | 1.7 | 0.3 | 15.9 |
| sample 3 | 69.0 | 25.0 | 1.8 | 0.0 | 0.8 | 1.3 | 1.9 | 38.3 |

Ridge, CO (presently manufactured by UIC, Inc., Joliet, IL). A complete description of the oxygen prepurification train, sample introduction port, quartz combustion tube, ovens, titration cell, and coulometer can be obtained from the manufacturer (UIC, Inc.) and the literature (Huffman, 1977; Johnson et al., 1985). Zero grade $O_2$ (99.6%) obtained from Linde Gases, East Chicago, IN, was used.

Before analysis of test samples, a background blank reading was obtained from the $CO_2$ coulometer. This reading was subtracted from that obtained when the actual samples were tested. During normal testing, four test strips attached to a preignited stainless steel rod were placed into the ambient temperature zone of the quartz combustion tube. The introduction port was sealed, and purified $O_2$ gas at a flow rate of about 100 cm³/min was allowed to purge the system for 60 s. The coulometer digital meter was set to zero, and the test strips were advanced into the first heated zone set at 450 ± 10 °C, for 5 min. Evolution of $CO_2$ generally ceased within 4.0–4.5 min. The samples were then advanced *in situ* into the second heated zone, set at 600 ± 10 °C, for 5 min (evolution of $CO_2$ ceased within 4.5–5.0 min). The digital display reading was recorded after a 5 min residence time in each zone. If only total carbon was desired, the samples were placed directly into the high-temperature zone for 5 min. The rationale and empirical data acquired for determining the aforementioned experimental conditions will be discussed in the Results and Discussion section.

**X-ray Photoelectron Spectroscopy Measurements.** Analyses were performed using an M-Probe XPS spectrometer manufactured by Fisons Surface Science, Mountain View, CA. The data system used was also supplied by the same manufacturer. The excitation source utilized monochromatic Al K-α (1486.6 eV) radiation focused to a 600 μm diameter beam. The base pressure of the spectrometer was $5 \times 10^{-10}$ Torr. The

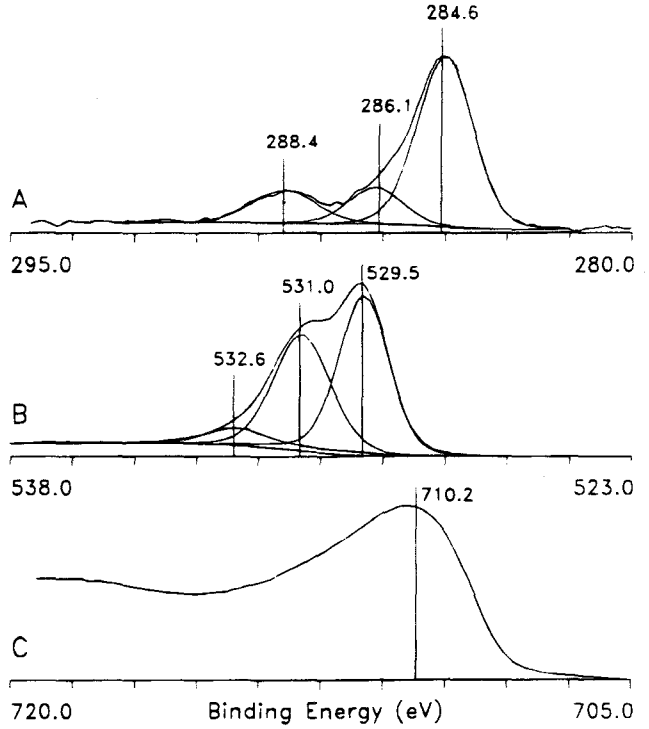


**Figure 1.** XPS (A) C 1s, (B) O 1s, and (C) Fe $2p_{3/2}$ spectral fits for alkaline-cleaned sample 1.

analyzer was operated with a 150 eV pass energy for the acquisition of survey spectra used for quantification and a 50 eV pass energy for acquisition of high-resolution core level spectra used to obtain chemical bonding information.

Quantification of survey data was accomplished by means of routines based on Scofield photoionization cross section values. To attain the O/Fe ratios, the high-resolution Fe $2p_{3/2}$ and O 1s core level spectral areas were measured utilizing a Shirley background subtraction. Measurement of the Fe $2p_{3/2}$ peak area included both the core line and the associated satellite. The elemental compositions reported in this paper are reproducible to within ±10%. High-resolution core level spectra were peak-fitted using a least-squares fitting routine which was allowed to iterate freely on the peak positions, integrated peak areas, and peak widths (fwhm). Core level spectra were referenced to the adventitious hydrocarbon contamination C 1s line observed at 284.6 eV or the Fermi edge, when carbon was not present. Binding energies quoted in this work are accurate to ±0.2 eV. The *in situ* XPS oxidation methodologies used to simulate the DOCC tests utilized a Model 04-800 reactor system manufactured by Perkin-Elmer, Physical Electronics Division, Eden Prairie, MN. The reactor was directly mounted to the sample preparation chamber of the M-Probe spectrometer. The base pressure of the preparation chamber was $1 \times 10^{-9}$ Torr. The base pressure of the reactor was $2 \times 10^{-8}$ Torr. The $O_2$ used in the reactor was 99.98% pure and was obtained from Matheson, Chicago, IL. Reactions were accomplished in 1 atm of $O_2$ successively at 450 and 600 °C using a flow rate of 100 cm³/min to mimic the coulometric experiment. Reacted samples were transferred directly into the XPS analyzer *in vacuo* after each treatment.

**Secondary Ion Mass Spectrometry.** SIMS analyses were performed using a PHI Model 6300 spectrometer manufactured by Perkin-Elmer Corporation, Physical Electronics Division, Eden Prairie, MN. The system

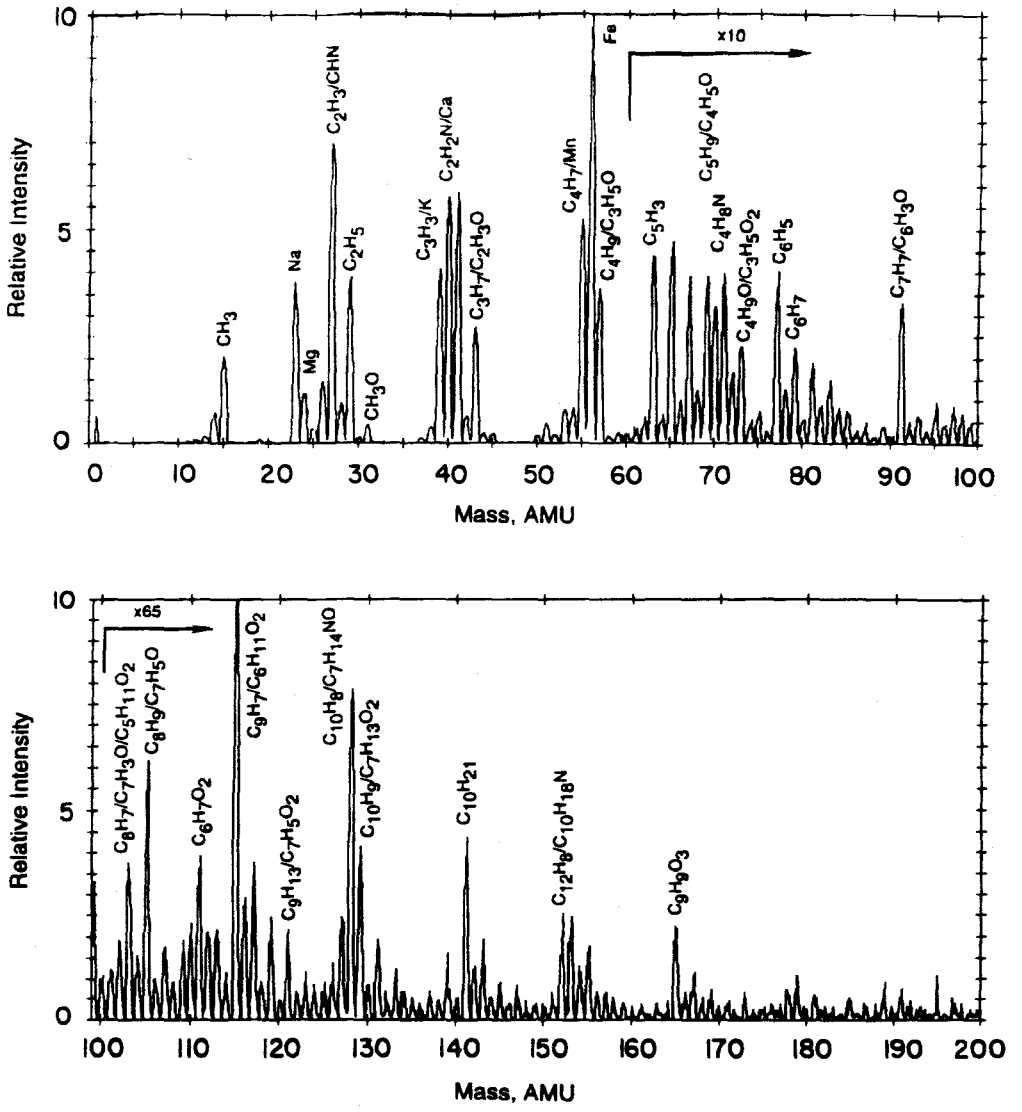


**Figure 2.** Positive static SIMS survey spectrum for alkaline-cleaned sample 3.

is equipped with a duoplasmatron microbeam ion gun, a 90° spherical sector energy analyzer, a Balzer's quadrupole mass analyzer, a continuous channel electron multiplier, and an Apollo host computer using PHI provided software. Utilizing local area networking technology and file transfer protocol, data files were moved from the Apollo workstation to the Inland Research VAX 6610. SIMS depth profile ratio curves were generated using resident RS/1 VAX software. The base pressure of the vacuum system was $2 \times 10^{-10}$ Torr. Positive static and dynamic SIMS surveys and SIMS depth profiles were conducted with a 7.0 keV xenon primary ion beam, on the alkaline cleaned and 450 and 600 °C DOCC analyzed samples. The primary ion beam dose for the static SIMS surveys was $3 \times 10^{12}$ ions/cm$^2$, which is below the critical ion dose for performing static SIMS analysis (Newman et al., 1991). For the dynamic SIMS survey and depth profile analyses, a focused 1.0 $\mu$A beam was rastered over a 2.25 or 0.25 mm$^2$ area, achieving primary ion beam current densities of 44 $\mu$A/cm$^2$ or 400 $\mu$A/cm$^2$, respectively, depending on the sputter rates desired. Secondary ions formed during depth profiling were 70% gated to prevent crater edge effects. For accurate depth profile calibration, crater depths were measured with a Talysurf 10 profilometer (Rank Taylor Hobson Limited, Leicester, England).

## Results and Discussion

**DOCC Measurements.** For differentiating organic from nonorganic carbon associated with steel contamination and processing, analytical conditions were chosen so as to preferentially oxidize the organic carbon and then the nonorganic carbon species present on the surface and near surface of the materials, respectively. Table 1 presents the results of the reactions of organic and nonorganic carbon containing substances with $O_2$ in the heated quartz combustion tube at 450 and 600 °C to form $CO_2$. These results show that virtually all of the organic samples reacted completely when tested in the 450 °C temperature zone and are consistent with the findings of Heistand and Humphries (1976), who also used the same conditions for the coulometric determination of organic carbon in shale. Nonorganic carbon containing species, on the other hand, reacted somewhat at 450 °C and more so at 600 °C. The carbon recovery observed for these species at 450 °C is assumed to be a combination of organic carbon contamination and possibly a small amount of the inorganic carbon that has reacted at this temperature. However, the majority of the inorganic carbon is reacted at the 600 °C temperature. Using a higher combustion temperature (650 °C) and air, Cadle et al. (1980) observed similar results when converting elemental carbon to $CO_2$ on

**Table 4. SIMS Analysis of Alkaline Cleaned CRS Samples**

| CRS | survey peak area ratios $CH_3^+/Fe^+$ [a] | survey peak area ratios $C^+/Fe^+$ [b] | total $C^+$ counts during profiling[b] |
|---|---|---|---|
| sample 1 | 0.10 | $2.7 \times 10^{-3}$ | $1.2 \times 10^3$ |
| sample 2 | 0.14 | $1.0 \times 10^{-2}$ | $2.1 \times 10^3$ |
| sample 3 | 0.41 | $1.4 \times 10^{-2}$ | $5.5 \times 10^3$ |

[a] Obtained with a $3.0 \times 10^{12}$ ions/cm$^2$ primary ion beam dose. [b] Obtained with a 44 $\mu$A/cm$^2$ beam current density.

diesel and industrial smokestack emission samples collected on glass fiber filter media. In addition, previous investigators have chosen 580–600 °C as the upper temperature limit for measuring total surface carbon on steel (Boggs and Pellissier, 1967; Lee and Lewis, 1970; King, 1978) and nickel (Solet, 1950). Upon increasing the temperature beyond this point, a continuous evolution of $CO_2$ with time was observed (Boggs and Pellissier, 1967; King, 1978). In addition, the diffusion coefficient of carbon in iron at this temperature is very low (Leslie, 1981); therefore the 600 °C temperature was chosen as the upper temperature limit for DOCC analysis of surface carbon on steel.

The DOCC results obtained from the sheet steel samples are summarized in Table 2. In each case the amount of carbon observed during the first stage measurements at 450 °C is slightly greater than that observed at 600 °C. This table reveals that, with respect to carbon, sample 1 is the cleanest steel with samples 2 and 3 having factors of approximately 2 and 4 times more carbon, respectively. These differences in carbon levels may be related to the different mill-processing histories for the three samples.

**Initial XPS and SIMS Surface Measurements.** The XPS quantitative results for the alkaline-cleaned samples 1–3 are presented in Table 3. The Mn and P observed are intrinsic to the type of steel analyzed, and the low amounts of Ca and N observed are probably from extraneous contamination, introduced during processing or sample preparation. Although an explicit comparison of these results to those obtained in the DOCC experiment cannot be made, the C/Fe elemental ratios given in Table 3 do follow the same trends (sample 1 < sample 2 < sample 3) as the total carbon results presented in Table 2. In using these ratios, the effects of the oxides and other elements are eliminated thereby simplifying interpretation of the XPS results.

Nearly identical high-resolution C 1s, O 1s, and Fe 2p spectra were observed on each surface. Some slight differences in the intensities of the components seen in the computer fits were observed; however, the binding energy positions of these components were nearly

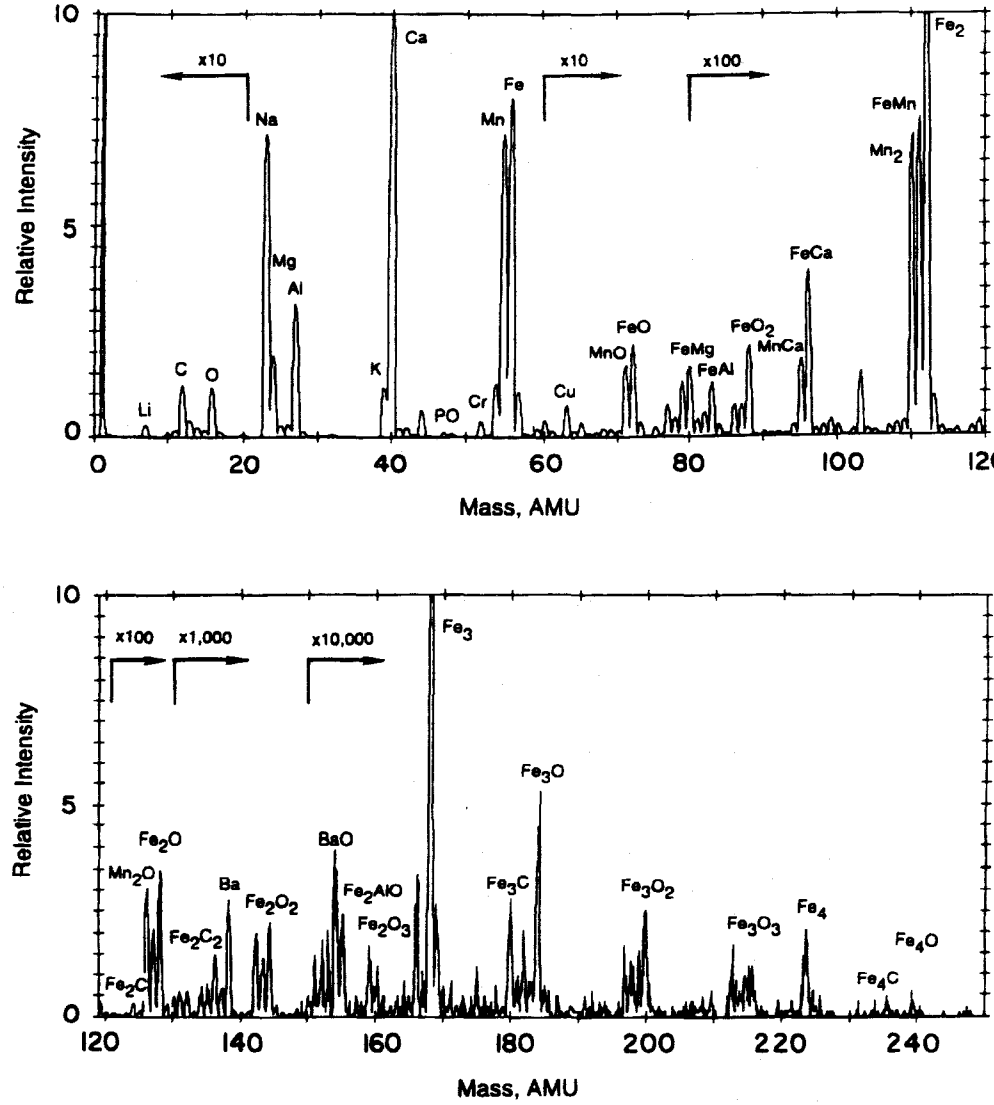


**Figure 3.** Positive dynamic SIMS survey spectrum acquired before depth profiling for sample 3.

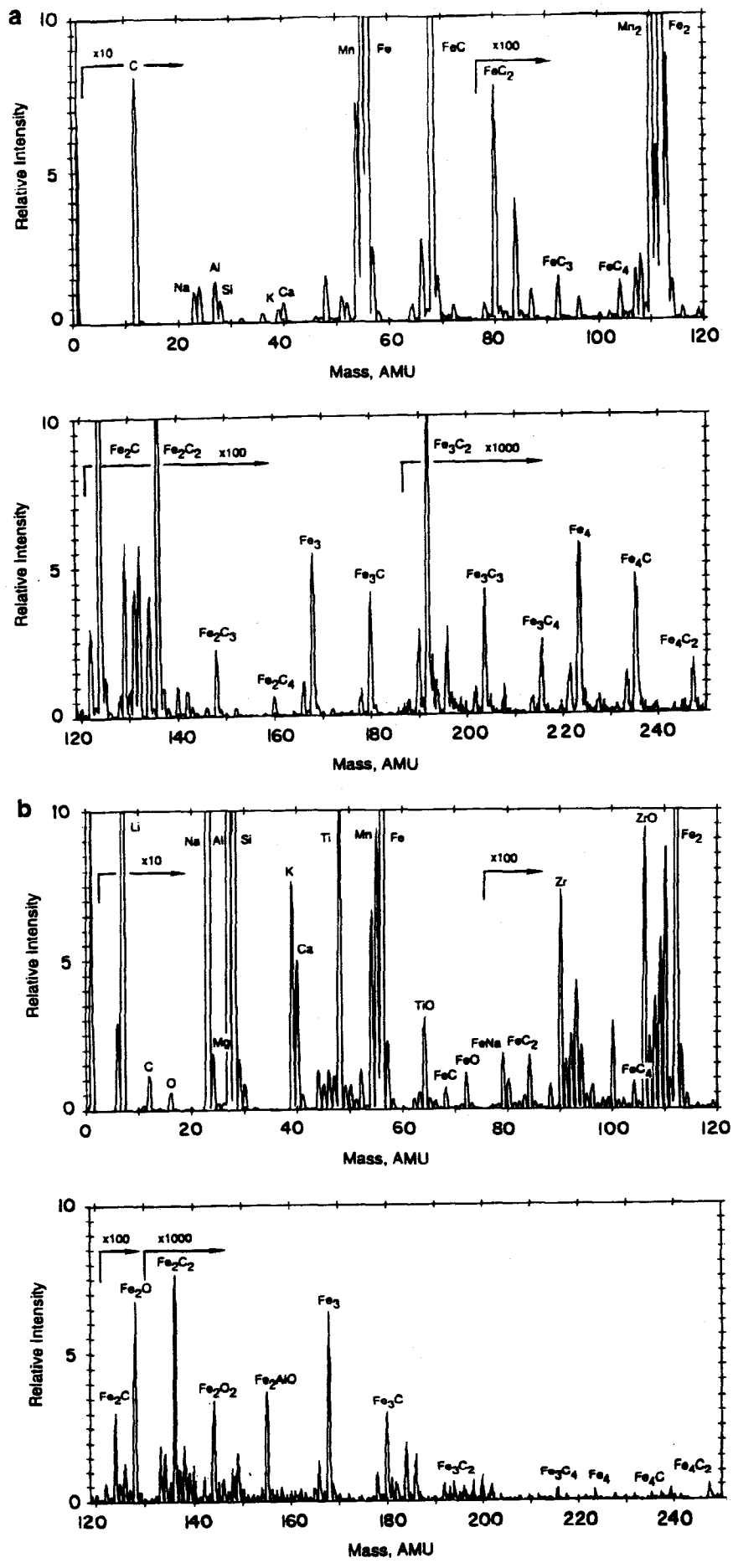


**Figure 4.** SIMS spectrum of (a) gray cast iron and (b) iron carbide.

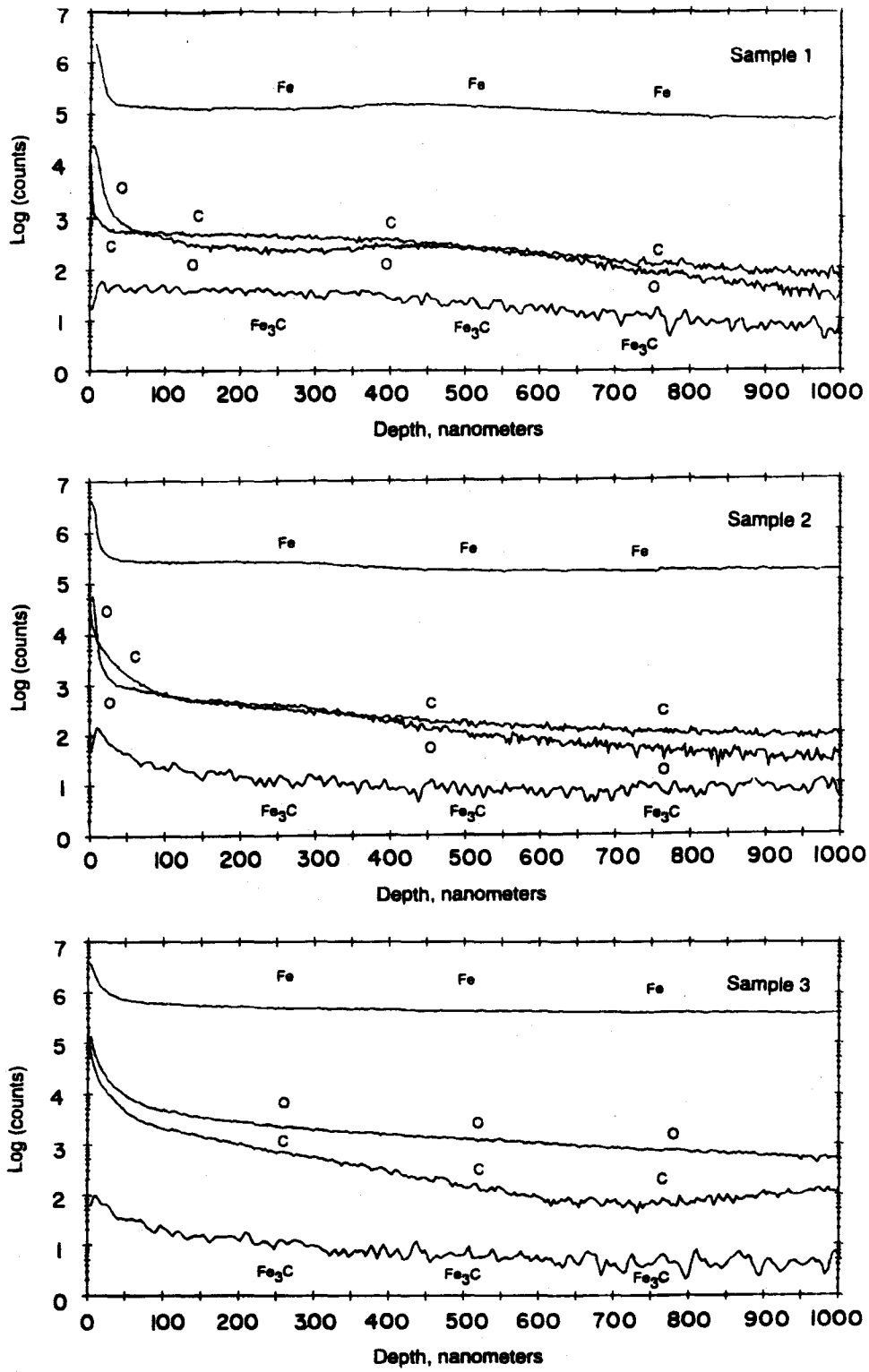


**Figure 5.** SIMS depth profiles for the alkaline-cleaned samples 1–3.

identical. Therefore, only the C 1s, O 1s, and Fe 2p spectral fits for sample 1, shown in Figure 1, are presented. The C 1s spectral fit (Figure 1a) reveals peaks at 284.6, 286.1, and 288.4 eV, which are attributed to aliphatic, ether, and carboxyl type carbons, respectively. These carbon species are probably a combination of contamination from the environment before insertion into the vacuum chamber, as well as contamination associated with the steel processing and cleaning. The O 1s spectrum (Figure 1b) reveals components at 529.5, 531.0, and 532.6 eV. The two strongest peaks at 529.5 and 531.0 eV are normally attributed to $Fe_2O_3$ and FeOOH, respectively (Schuetzle et al., 1994). The remaining O 1s peak at 532.6 eV is most likely associated with the carboxyl carbon observed in the C 1s spectrum. The intrinsic broadness of the Fe 2p spectrum (Figure 1c) does not allow for an accurate computer fit to confirm the presence of $Fe_2O_3$ and FeOOH states observed in the O 1s spectrum. The main peak envelope, however, appears at 710.2 eV,

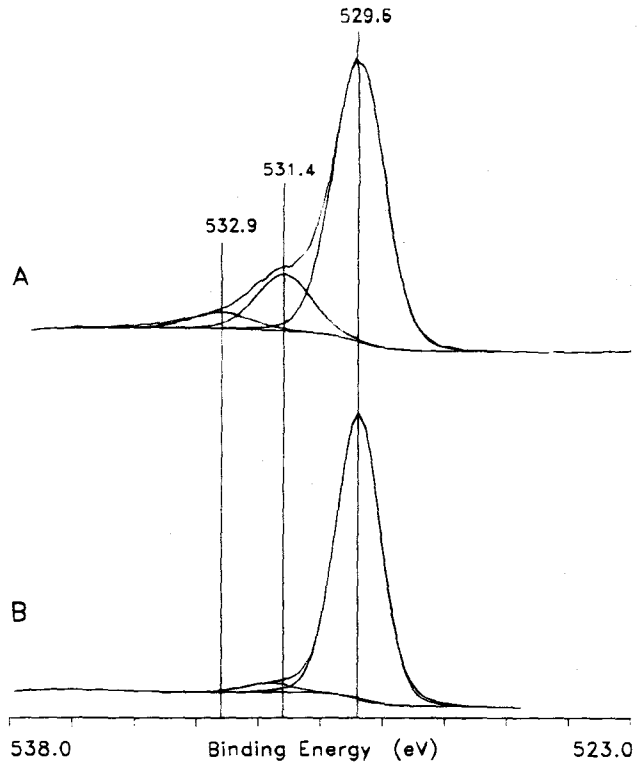


**Figure 6.** XPS O 1s spectra for sample 1 acquired after (A) coulometer and (B) *in situ* treatments.

**Table 5. XPS Quantitative Results after 450 °C DOCC Analysis and *in Situ* Oxidation Treatment**

| CRS | method | composition (at. %) C | O | Fe | N | Mn | Cl | Na | C/Fe ratio |
|---|---|---|---|---|---|---|---|---|---|
| 1 | DOCC | 42.0 | 47.0 | 10.0 | 1.1 | 0.0 | 0.0 | 0.0 | 4.2 |
| 2 | DOCC | 39.0 | 48.0 | 10.0 | 3.0 | 0.3 | 0.0 | 0.0 | 3.9 |
| 3 | DOCC | 43.0 | 45.0 | 8.7 | 2.5 | 1.2 | 0.0 | 0.0 | 4.9 |
| 1 | *in situ* oxidation | 0.0 | 76.0 | 19.0 | 0.0 | 0.0 | 3.1 | 1.9 | 0.0 |
| 2 | *in situ* oxidation | 0.0 | 75.0 | 21.0 | 0.0 | 0.0 | 2.0 | 1.5 | 0.0 |
| 3 | *in situ* oxidation | 0.0 | 73.0 | 19.0 | 0.0 | 2.7 | 2.1 | 2.9 | 0.0 |

which is normally associated with $Fe_2O_3$. A metallic Fe state, normally observed at 706.8 eV, would have been resolvable in these spectra.

The positive static SIMS survey spectrum for the alkaline-cleaned CRS sample 3 is shown in Figure 2. The SIMS spectra for samples 1 and 2 were similar, with differences observed mainly in peak intensities. Common to all of the static SIMS spectra were predominant organic fragments, which can be grouped as aliphatic, aromatic, oxygen-containing, and nitrogen-containing species. Several inorganic species were also observed. Multiple peak assignments were made in some cases since some SIMS peaks may be the resultant combination of two or more ionic species occurring at the same mass within the resolving power of the instrument. These interpretations are based on previously published data (Newman et al., 1991) and are consistent with the functional groups and elements identified by XPS (see Figure 1 and Table 3). The static SIMS $CH_3^+/Fe^+$ peak area ratios for the three alkaline-cleaned CRS samples, shown in Table 4, follow the same trend as those observed from the DOCC and XPS organic carbon measurements. The organics are most likely due to residual rust preventative oil, cleaner surfactant, and adventitious carbon.

**SIMS Depth Profile Analysis.** Figure 3 shows the positive ion dynamic SIMS survey spectrum obtained before SIMS depth profiling for sample 3. It should be noted that this spectrum is not static in nature, such as the spectrum presented in Figure 2, due to the higher current density used. Consequently, the high-mass peaks observed in this spectrum originate deeper than those observed at low mass, and increased fragmentation of molecular species occurs. Therefore the spectrum presented in Figure 3 reveals more information of the underlying oxide. SIMS dynamic survey spectra for samples 1 and 2 were qualitatively similar to that for sample 3. The $C^+/Fe^+$ peak area ratios obtained from the dynamic SIMS surveys, before profiling, for the three CRS samples as shown in Table 4, follow the same total surface carbon level trends as those obtained from DOCC analysis. Observed in Figure 3, as well as in the XPS data presented in Table 3, is the presence of salts and oxides of alkali, alkaline earth, and transition metals. These substances have been shown by another investigator (McKee, 1981) to catalyze the combustion reactions of carbon.

Carbon existing in the bulk of batch annealed steel is known to be predominantly iron carbide (cementite) in nature. To verify that the iron carbide fragments observed in Figure 3 were indeed due to the cementite in the steel, XPS spectra of these samples were acquired and compared to spectra acquired on iron carbide powder. These results, not shown, revealed a low binding energy C 1s peak at 283.4 eV, generally accepted as carbidic carbon, on both the samples and standard surfaces, thus confirming the presence of iron carbide on these materials. The SIMS spectrum of gray cast iron as shown in Figure 4a reveals a homologous series of iron carbide fragments corresponding to the $Fe_xC_y^+$ species. The SIMS spectrum of the iron carbide reference material (Figure 4b) revealed titanium and zirconium impurities; however, the majority of the iron carbide peaks observed in gray cast iron were also present in this spectrum. In each case, the $Fe_xC_y+$ species observed in Figure 4 parts a and b correlates well with those observed in Figure 3.

SIMS depth profiles for $C^+$, $O^+$, $Fe^+$, and $Fe_3C^+$ were obtained in order to follow the behavior of carbon and iron oxide as a function of depth. Profiles for the alkaline-cleaned samples 1–3, to a depth of about 1000 nm, are shown in Figure 5. The observed profile differences for these three samples are attributed to the different processing conditions used during steel manufacturing. The $O^+$ signal decreased steadily yet did not reach baseline in each profile. The total SIMS $C^+$ profile counts are lowest for sample 1 and highest for sample 3, as shown in Table 4. The $C^+$ profiles in Figure 5 reveal the thinnest carbon layer to be on sample 1 and the thickest carbon layer to be on sample 3. These observations are consistent with previous discussions.

The origin of some of the carbon in the $C^+$ profiles presented in Figure 5 may be due to cementite, as revealed by the $Fe_3C^+$ profiles. However, the cementite cannot account for all the carbon present since the $C^+$ and $Fe_3C^+$ profiles do not parallel one another near the surface. A comparison of the $C^+/Fe_3C^+$ profile ratios (data not shown) revealed that the $C^+$ profiles do not coincide with the corresponding $Fe_3C^+$ profiles to a depth of about 40 nm for sample 1, 400 nm for sample 2, and 550 nm for sample 3. This discrepancy may be attributed to the presence of amorphous carbon. This would be consistent with past investigations where X-ray diffraction analysis of soot (elemental amorphous carbon resulting from the thermal cracking of organic tandem rolling oils in a reducing annealing atmosphere)

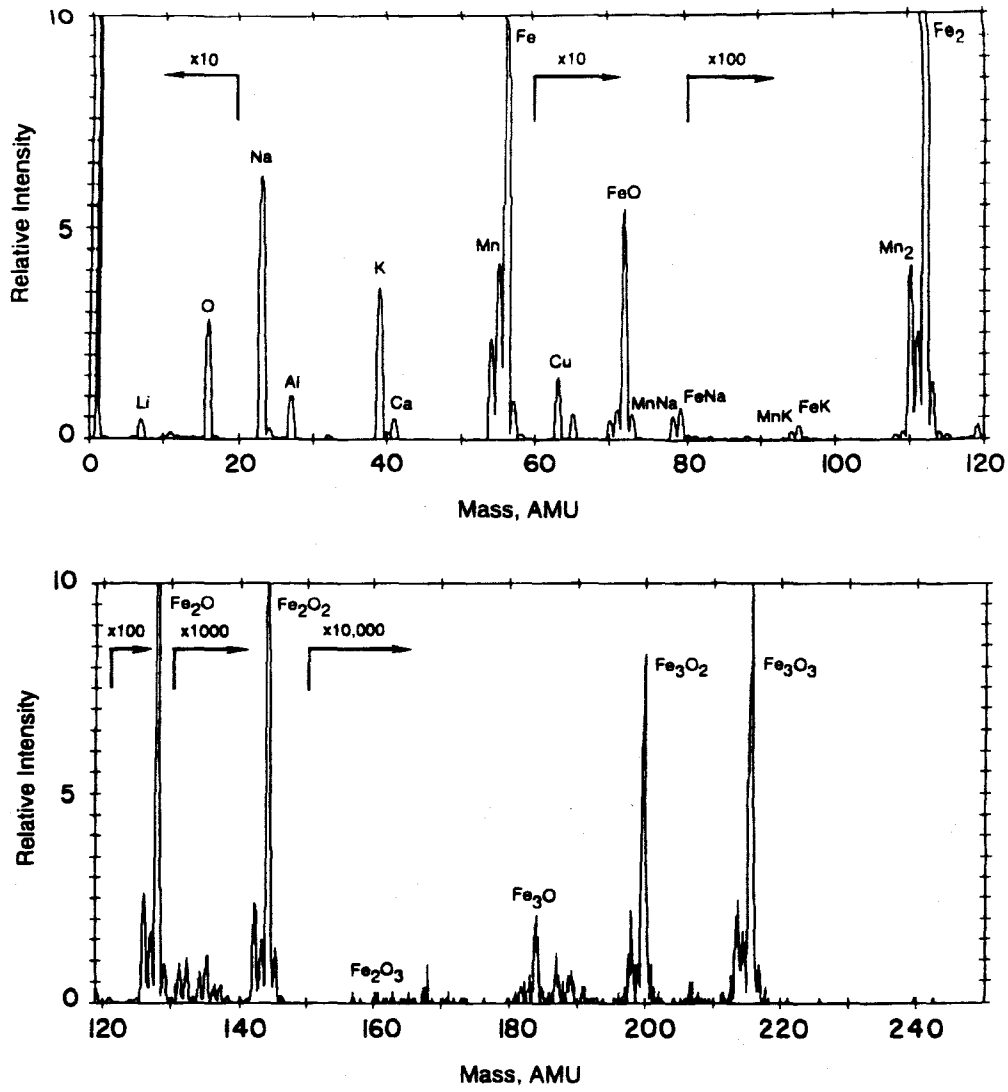


**Figure 7.** SIMS survey spectrum obtained before depth profiling on the 450 °C DOCC treated sample 3.

**Table 6. XPS Quantitative Results after 600 °C DOCC Analysis and *in Situ* Oxidation Treatment**

| CRS | Method | composition (at. %) C | O | Fe | N | Mn | Cu | Na | C/Fe ratio |
|---|---|---|---|---|---|---|---|---|---|
| 1 | DOCC | 38.0 | 49.0 | 10.0 | 1.8 | 0.5 | 0.0 | 0.0 | 3.8 |
| 2 | DOCC | 40.0 | 47.0 | 9.6 | 2.1 | 0.0 | 1.7 | 0.0 | 4.2 |
| 3 | DOCC | 39.0 | 46.0 | 8.9 | 2.6 | 2.4 | 0.9 | 0.0 | 4.4 |
| 1 | *in situ* oxidation | 0.0 | 75.0 | 19.0 | 0.0 | 0.0 | 6.5 | 0.0 | 0.0 |
| 2 | *in situ* oxidation | 0.0 | 77.0 | 19.0 | 0.0 | 0.0 | 2.4 | 1.7 | 0.0 |
| 3 | *in situ* oxidation | 0.0 | 72.0 | 16.0 | 0.0 | 3.4 | 4.7 | 0.0 | 0.0 |

on CRS samples revealed an amorphous carbon band (Iezzi and Leidheiser, 1981; Leroy et al., 1984). Even though some investigators have reported the formation of graphite during certain annealing conditions (Inokuti, 1975; Leroy et al., 1976), the annealing conditions used to produce these steels did not allow for the formation of surface graphite.

**XPS and SIMS Measurements of Samples 1–3 after the 450 °C DOCC Analysis and *in Situ* Oxidative Treatments.** Each of the three alkaline-cleaned steel surfaces were analyzed by XPS after being subjected to the 450 °C DOCC analysis and *in situ* oxidative treatment at 450 °C. Table 5 compares the XPS results after these treatments. Since the amounts of carbon present on the samples analyzed by XPS after the 450 °C DOCC measurement are nearly the same and no carbon was detected after the 450 °C *in situ* treatment, the carbon detected after the DOCC experiments was probably adventitious contamination. All of the carbon observed by XPS and static SIMS analyses prior to DOCC testing was previously shown to be primarily organic in nature (Figures 1a,b and 2). These results are in good agreement with Table 1 in that all the organic species should be removed after the 450 °C DOCC treatment. The Mn also observed in Table 5 represents a constituent in the steel, as was observed on the virgin surfaces, and the Cl and Na may represent contamination introduced during steel processing which surface segregates upon treatment. The Na and Cl were only observed on the *in situ* treated materials and not the DOCC treated materials. The reason for this is unclear but may be explained by the adventitious carbon layer observed on the DOCC materials actually masking any surface segregated material such as Na and Cl.

Comparison of the high-resolution XPS spectra acquired on each of the samples after both DOCC and *in situ* 450 °C treatments again revealed no significant differences between steels. The O 1s spectra for sample 1 acquired after both coulometer and *in situ* treatments are given in Figure 6. Both these spectra reveal a dominant peak at 529.6 eV, assigned to $Fe_2O_3$. The hydroxide peak previously seen in Figure 1b has been considerably reduced in the spectrum acquired after the DOCC treatment (Figure 6a) and has completely disap-

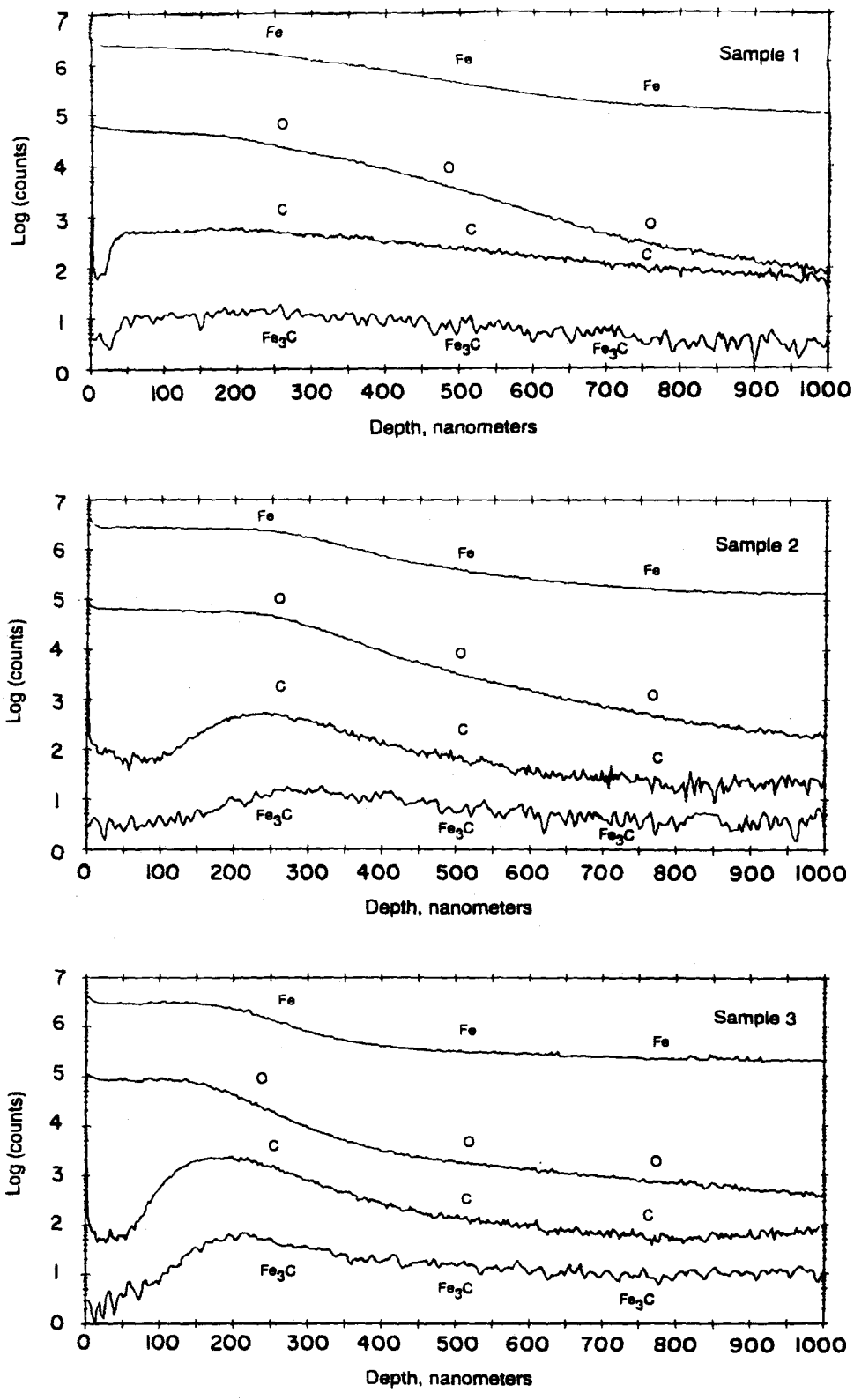


**Figure 8.** SIMS depth profiles for 450 °C DOCC treated samples 1–3.

peared in the spectrum acquired after the *in situ* treatment (Figure 6b). The absence of carbon observed in the survey spectra (Table 5) substantiates the disappearance of the carboxyl O 1s species (532.9 eV) in Figure 6b. There is, however, a minor carboxyl peak in Figure 6a, which would correlate to the adventitious carbon seen in the C 1s survey results. The identity of the low-intensity peak (531.7 eV) also observed in Figure 6b is not known at this time; however, it might be an additional oxide species present after the *in situ* treatment. The Fe 2p spectra (not shown) all revealed a broad envelope at 710.2 eV identical to that observed on the virgin samples and previously defined as $Fe_2O_3$.

The absence of FeOOH observed after the *in situ* treatments of the samples shown in Figure 6b would suggest that only $Fe_2O_3$ was present on these surfaces. However, the O/Fe observed ratio for all the *in situ* samples was approximately 3.8, substantially greater than the stoichiometric ratio of 1.5. Subsequent experiments were undertaken to define the O/Fe ratio of a

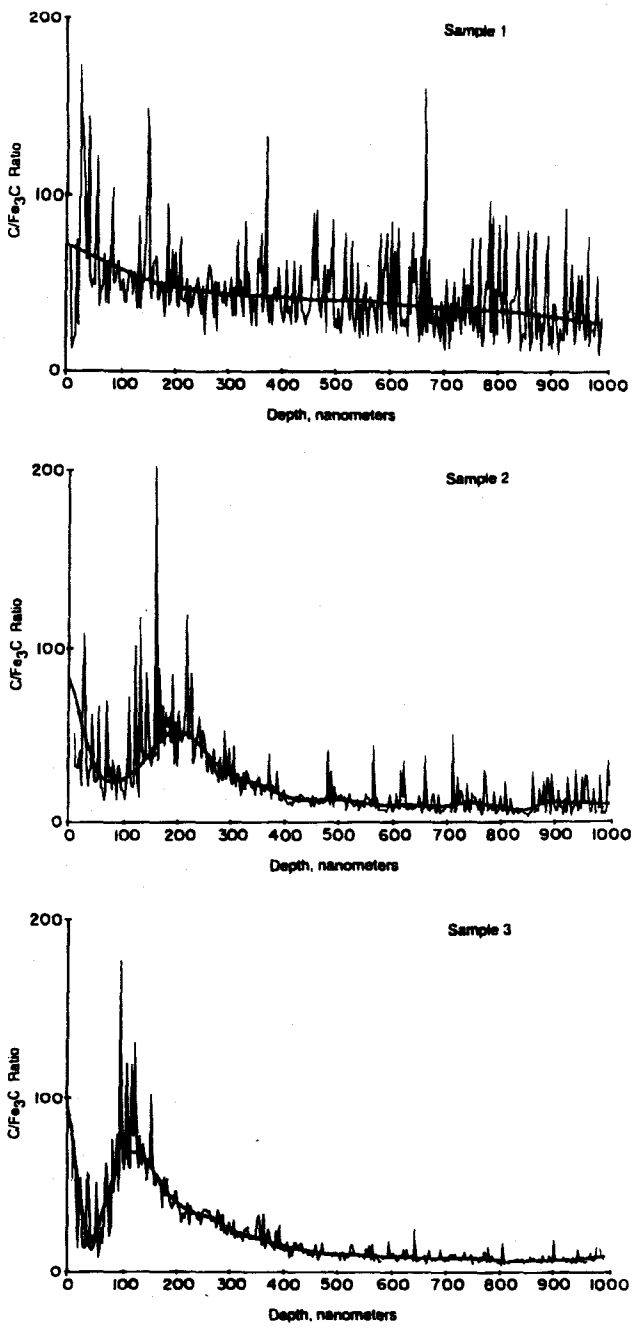


**Figure 9.** SIMS depth profile $C^+$ to $Fe_3C^+$ ratio curves for samples 1–3.

$Fe_2O_3$ powder standard and an oxidized Fe foil before and after *in situ* oxidation. In each of these experiments the O/Fe was again approximately 3.8. Therefore, it is reasonable that the 3.8 O/Fe ratio observed after the *in situ* treatments is representative of $Fe_2O_3$. The discrepancy of the theoretical and empirical ratios could be the result of inaccurate quantification due to the intrinsically broad and asymmetric shape of the Fe 2p peak or inaccurate sensitivity factors used to quantify these spectra.

A SIMS survey spectrum obtained before depth profiling on the 450 °C DOCC treated sample 3 is shown in Figure 7. SIMS survey spectra for the 450 °C DOCC treated samples 1 and 2 were qualitatively similar to that for sample 3. Revealed in this spectrum are significant increases in the intensities of the iron oxide fragments $FeO^+$, $Fe_2O^+$, $Fe_2O_2^+$, $Fe_3O^+$, $Fe_3O_2^+$, and $Fe_3O_3^+$, along with the disappearance of the $Fe_3^+$ and $Fe_4^+$ molecular iron ion fragments, as compared to the virgin surface survey (Figure 3). This indicates a greater degree of iron oxidation, consistent with previously discussed XPS results.

The $Fe^+$ and $O^+$ profiles of the 450 °C DOCC treated samples revealed a gradual decrease in the oxygen content for each of the samples, suggesting a fairly thick oxide layer (Figure 8). Following the removal of the adventitious carbon, a low carbon signal is present in the oxide layer of all three samples. As the oxide layer is sputtered away, the $C^+$ profiles begin to rise and achieve maximum intensity at the newly formed oxide/metal interfaces. These results indicate that all the surface carbon has been removed after the 450 °C treatment as well as a certain amount of the underlying near surface carbon. Analogous to the alkaline-cleaned samples, part of carbon underlying the $Fe_2O_3$ layer can be attributed to cementite, as revealed by the $Fe_3C^+$ profiles in Figure 8. However, a comparison of the $C^+$ to $Fe_3C^+$ profile ratio curves (Figure 9) reveals that to a depth of about 550 nm carbon other than cementite, probably amorphous carbon, also exists.

From the carbon and oxygen profiles it is apparent that besides surface organic carbon, a mixture of amorphous carbon and cementite, both inorganic carbon species, is combusted and measured at the near surface during the 450 °C oxidation step. An upper limit to the amount of inorganic carbon consumed can be estimated by assuming that the bulk carbon composition is homogeneous and that during oxidative treatment this additionally measured inorganic carbon evolves from the newly formed $Fe_2O_3$ layer. The average depth of the iron oxide layer formed for the three samples is about 200 nm (determined where the $C^+$ reaches maximum intensity). The amount of carbon combusted during formation of the 200 nm oxide layer, assuming a bulk carbon content of 0.06 wt % and a pure $Fe_2O_3$ layer with a density of 5.24 g/$10^{-6}$ $m^3$, normalized to an area 1 $m^2$ (the units of measurement of the DOCC technique) is calculated as

$$\text{mg of C} = \left(\frac{0.6(\text{mg of C})}{0.9994(\text{g of Fe})}\right)\left(\frac{55.8(\text{g of Fe})}{79.8(\text{g of FeO}_{1.5})}\right) \times \left(\frac{5.24(\text{g of FeO}_{1.5})}{10^{-6}\ \text{m}^3}\right)(200 \times 10^{-9}\ \text{m}^3)$$

The amount of carbon combusted is calculated to be 0.440 mg. Consequently, the amount this measurement would contribute to the 450 °C DOCC measurements given in Table 2 is 17.1%, 10.8%, and 4.50% for samples 1, 2, and 3, respectively. Clearly in all cases the majority of carbon measured at 450 °C is from the uppermost surface, i.e., not inorganic carbon combusted from the bulk. However, the near surface inorganic carbon contribution, percentage-wise, becomes more significant for cleaner steels, i.e., sample 1.

**XPS and SIMS Measurements of Samples 1–3 after the 600 °C DOCC Analysis and *in Situ* Oxidative Treatments.** The XPS quantitative results of the steel samples after the 600 °C DOCC treatment and *in situ* oxidation are given in Table 6. No detectable carbon was observed on these samples after the 600 °C *in situ* treatment. The XPS results after both the DOCC and *in situ* treatments are nearly identical to the corresponding results seen in Table 5 after the 450 °C treatments. The carbon observed after the 600 °C DOCC treatment can again be attributed to contamination from atmospheric exposure. The high-resolution core level spectra acquired after both 600 °C treatments are essentially identical to those acquired after the 450

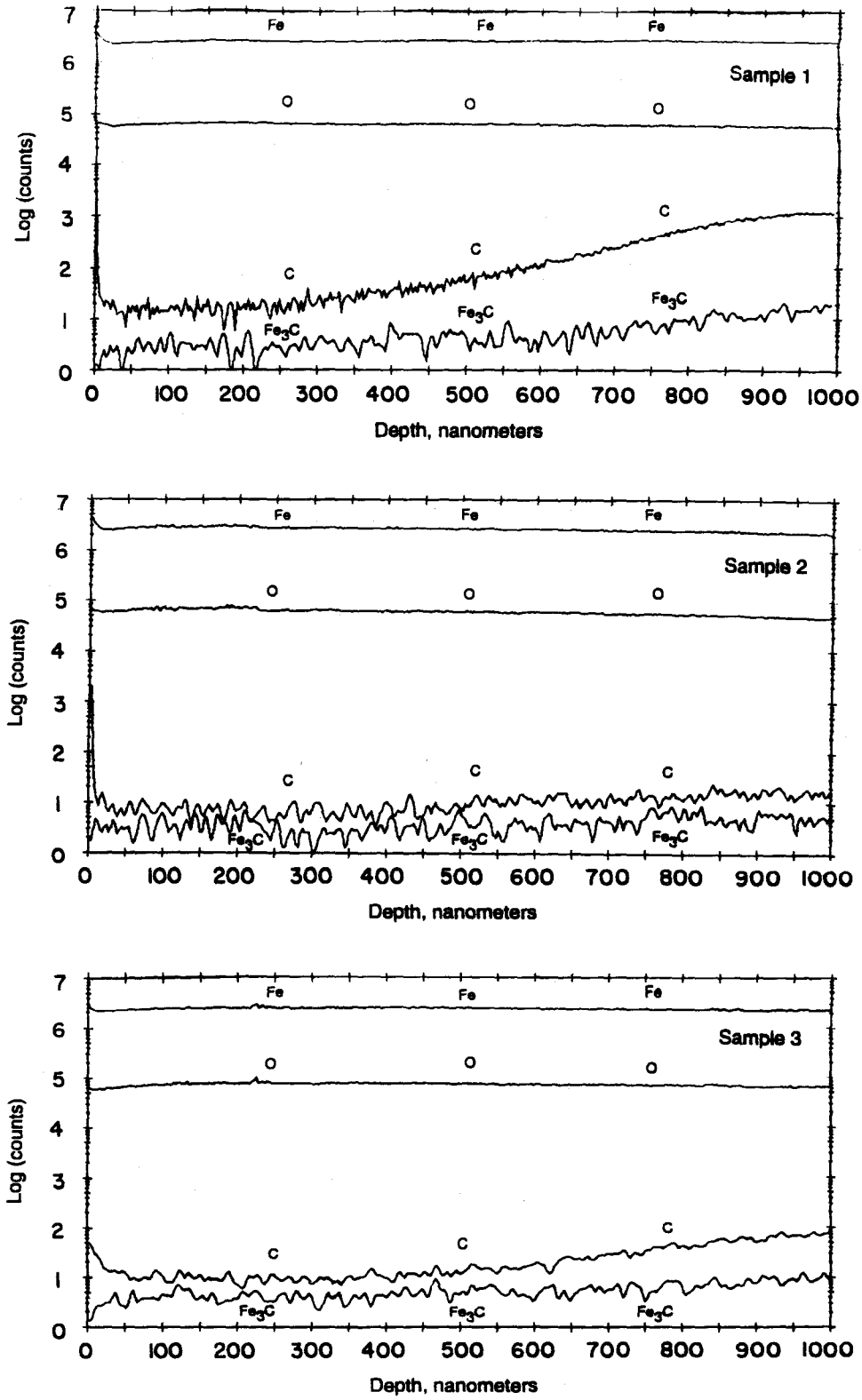


**Figure 10.** SIMS depth profiles for 600 °C DOCC treated samples 1–3.

°C treatments. The observed copper shown in Table 6 (also shown in the SIMS spectra of Figures 3 and 7) is intrinsic to the steel analyzed and surface segregated after treatment.

Figure 10 shows the $Fe^+$, $O^+$, $C^+$, and $Fe_3C^+$ SIMS depth profiles for the three DOCC 600 °C heat treated samples. The $O^+$ and $Fe^+$ profiles for these samples show an increase in the thickness of the oxide layer, as compared to the 450 °C heat treated samples. After the removal of the adventitious carbon, the $C^+$ and $Fe_3C^+$ signals are near the detection limits of the instrument, to a depth of about 400 nm within the oxide layers. Thus, compared to the 450 °C treatment, the near surface carbon was combusted to a considerably greater depth. At about 400 nm, the carbon profiles begin to rise with a simultaneous increase in the $Fe_3C^+$ signal. Under the sputtering conditions used, it was impractical to determine information beyond 1000 nm.

To obtain the oxide thickness and examine the behavior of carbon beneath this oxide layer, depth

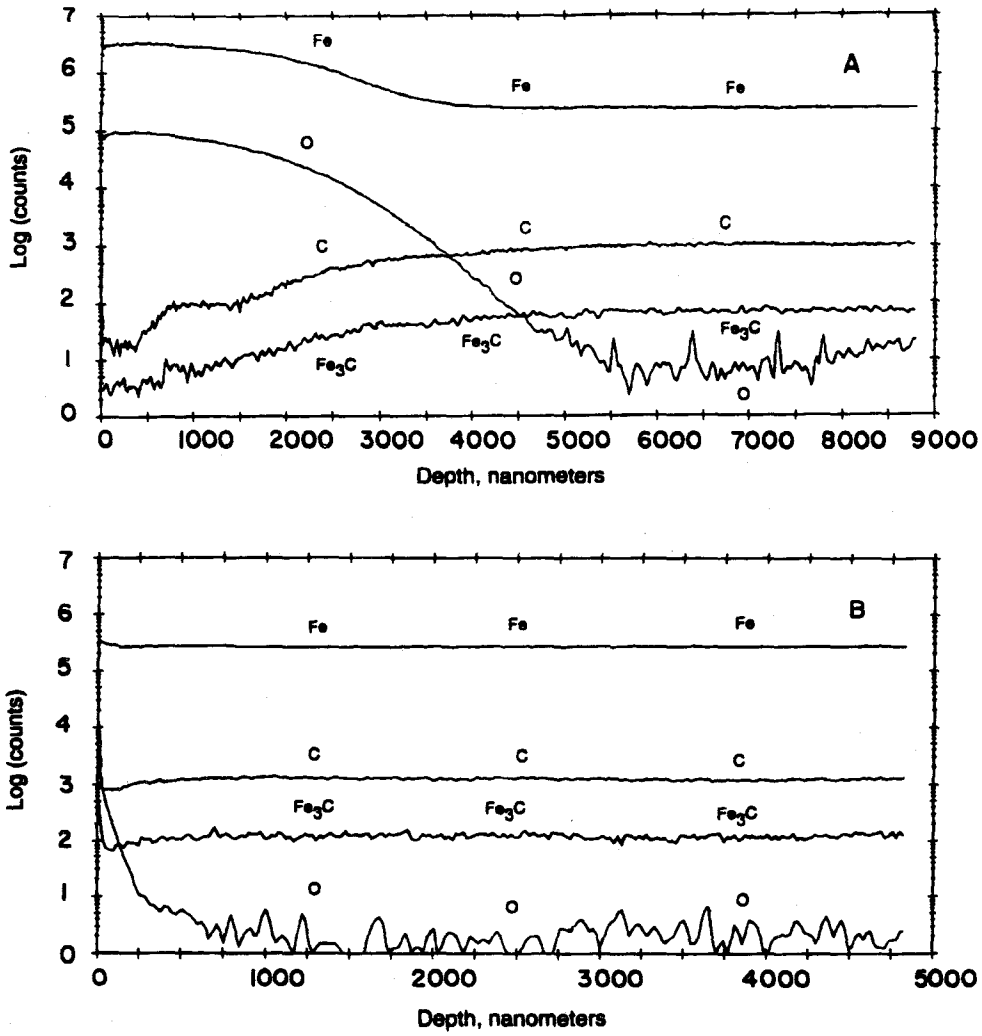


**Figure 11.** SIMS depth profiles for (A) 600 °C DOCC treated and (B) polished sample 3 at higher primary ion beam current densities.

profiles were acquired utilizing a nearly 10-fold increase in the primary ion beam current density, from 44 to 400 $\mu A/cm^2$. This higher sputtering rate enabled profiling through the oxide layer as well as reaching steady state bulk compositional profiles. To verify that bulk steady state compositions were reached, the virgin surface of sample 3 was metallographically polished (1 $\mu$m diamond paste) in order to eliminate the inherent surface oxide and surface carbon from the sample. Figure 11 parts a and b show the higher primary ion beam current density SIMS depth profiles for the 600 °C DOCC heat treated and polished sample 3, to depths of about 9000 and 5000 nm, respectively. From a depth of about 5000 to 9000 nm the shapes and magnitudes of the $Fe^+$, $O^+$, $C^+$, and $Fe_3C^+$ profiles match those of the polished sample (Figure 11b), indicating that bulk iron, oxygen, carbon, and iron carbide have been reached. From 400 to 5000 nm (Figure 11a) there is a steady increase in the $C^+$ signal, with a concomitant increase in the $Fe_3C^+$ signal, as verified by $C^+/Fe_3C^+$ profile ratioing. At 5000 nm bulk steady state composition is reached and the $C^+$ and $Fe_3C^+$ profiles continue to parallel one another. These results indicate that the observed carbon beginning at 400 nm in the oxide layer and continuing into the bulk steel is cementite.

Figure 11a shows that the $Fe_2O_3$ layer formed during the 600 °C DOCC oxidative treatment is about 2000 nm thick. Using the same assumptions as for the 450 °C oxidation step, the amount of inorganic carbon combusted within this layer is estimated to be 4.40 mg, i.e., 10 times that combusted at 450 °C. Although the nonorganic carbon measured at 600 °C for sample 3 (see Table 2) was more than twice the calculated 4.40 mg, the DOCC measurement for sample 2 was close to the calculated value, while the measurement for sample 1 was considerably less than this estimate. Variables associated with the estimate are iron oxide thickness and bulk carbon content. Fluctuations in steel surface roughness can add error in determining depth measurements by SIMS depth profiling. Most importantly though, the near surface carbon content is not necessarily homogeneous as a function of depth and may not be reflective of the bulk composition. The XPS results showed that all surface carbon is combusted at 450 °C oxidation. Thus, the 600 °C DOCC carbon measurement must be comprised entirely of near surface inorganic carbon.

## Conclusions

Cold-rolled steel surfaces were characterized by XPS and SIMS before and after DOCC analysis in order to (1) obtain a better understanding of the types of surface carbon present on CRS, (2) characterize the combustion of adventitious and native carbon during the two temperature stage DOCC analysis procedure, and (3) determine the type and depth of the oxide layers formed.

XPS and static SIMS analyses of the alkaline-cleaned steels prior to DOCC treatment revealed that the

surfaces were dominated by organic carbon species resulting from the presence of processing oils and adventitious contamination. Dynamic SIMS profiles revealed the presence of cementite and amorphous carbon species beneath the surface and well into the iron matrix.

XPS data were acquired on samples subjected to the first stage of the DOCC analysis (5 min at 450 °C) and identical samples subjected to the corresponding *in situ* treatment. These analyses revealed that all organic carbon was oxidized to $CO_2$ after the first stage of the DOCC experiment. Dynamic SIMS depth profiles, also acquired on samples subjected to the first stage of the DOCC analysis, revealed that a portion of the near surface inorganic carbon, expelled and combusted during formation of $Fe_2O_3$, was measured as well. This amount of inorganic carbon is minor, but its contribution becomes more significant on cleaner steels. The second stage of the DOCC analysis (an additional 5 min at 600 °C) was attributed entirely to near surface inorganic carbon, measured to a sample depth of approximately 2000 nm.

XPS and SIMS quantitative results followed the same surface carbon level trends as those observed from the 450 °C DOCC analysis, which confirms that the DOCC measurement detects primarily the same organic surface carbon as observed by these surface analytical techniques. The 600 °C DOCC treatment obviously probes deeper than what is attainable by these surface techniques unless depth profiling is utilized. However, the determination of near surface inorganic carbon can yield a greater insight into the effects of the mill-processing conditions used to manufacture the steel.

The results of this study indicate that the complementary DOCC, XPS, and SIMS techniques employed show promise in characterizing surface and near surface carbon found in steels that undergo different production practices.

## Literature Cited


Boggs, W. E.; Pellissier, G. E. The Determination of Organic Carbon on the Surface of Steel Sheets. *Mater. Res. Stand.* **1961**, *1*, 627–630.

Cadle, S. H.; Groblicki, P. J.; Stroup, D. P. Automated Carbon Analyzer for Particulate Samples. *Anal. Chem.* **1980**, *52*, 2201–2206.

Coduti, P. L. Effect of Residual Carbon on the Paintability of Steel Strip. *Met. Finish.* **1980**, *78*, 51–57.

Coduti, P. L. Relationship of the Surface Cleanliness and Surface Chemistry to the Corrosion Performance of Painted HSLA Steels for Exposed Automotive Applications. In *Automotive Corrosion by Deicing Salts*; Baboian, R., Ed.; National Association of Corrosion Engineers: Houston, TX, 1981; pp 363–376.

Coduti, P. L. Effect of Steel Processing on the Surface Carbon of Cold-Rolled Steel. In *Technological Impact of Surfaces*; American Society for Metals: Metals Park, OH, 1982; pp 57–101.

Coduti, P. L.; Earl, D. E. Cleanliness Measurement Techniques on Sheet Steel Surfaces. In *Proceedings of the 41st Porcelain Enamel Institute Technical Forum*; The American Ceramic Society, Inc.: Columbus, OH, 1980; pp 167–172.

Coduti, P. L.; Smith, D. E. How Clean is Clean - A Technical Evaluation of Cleanliness. In *Proceedings of the National Coil Coaters Association*; National Coil Coaters Association: Chicago, IL, 1979; pp 9–12.

*Fisher, T. W.; Iezzi, R. A.; Madritch, J. M. Theoretical and Practical* Considerations of Sheet Steel Surface Cleanliness; SAE Technical Paper Series 800149; Society of Automotive Engineers, Inc.: Warrendale, PA, 1980; pp 1–13.

Heistand, R. N.; Humphries, H. B. Direct Determination of Organic Carbon in Oil Shale. *Anal. Chem.* **1976**, *48*, 1192–1194.

Hospadaruk, V.; Huff, J.; Zurilla, R. W.; Greenwood, H. T. Paint Failure, Steel Surface Quality and Accelerated Corrosion Testing; SAE Technical Paper Series 780186; Society of Automotive Engineers, Inc.: Warrendale, PA, 1978; pp 1–7.

Huffman, E. W. D., Jr. Performance of a New Automatic Carbon Dioxide Coulometer. *Microchem. J.* **1977**, *22*, 567–573.

Iezzi, R. A.; Leidheiser, H., Jr. Surface Characteristics of Cold-Rolled Steel as They Affect Paint Performance. *Corrosion (Houston)* **1981**, *37*, 28–38.

Inokuti, Y. Formation of Graphite on the Surface of Cold Rolled Low Carbon Steel Sheet During Annealing. *Trans. ISIJ* **1975**, *15*, 314–323.

Johnson, K. M.; King, A. E.; Sieburth, J. M. Coulometric $TCO_2$ Analysis for Marine Studies; An Introduction. *Marine Chem.* **1985**, *16*, 61–82.

King, A. E. Direct Determination of Carbon on Metal Surfaces; The Association for Finishing Processor Technical Paper FC78-584; Society of Manufacturing Engineers: Dearborn, MI, 1978, pp 1–9.

Lee, W. H.; Lewis, L. L. Determination of Carbon in Thin Films on Steel Surfaces. *Anal. Chem.* **1970**, *42*, 103–106.

Leroy, V.; Richelmi, J.; Graas, H. Graphite Formation on the Surface in Annealed Low Carbon Steel Sheet. *Metal. Rep. CRM* **1976**, *49*, 49–58.

Leroy, V.; Servais, J. P.; Chatelain, B. Surface Analysis Applied to Cold Rolled Steel Sheets. In *Secondary Ion Mass Spectrometry SIMS IV*; Benninghoven, A., Okano, J., Shinizu, R., Werner, H. W., Eds.; Springer-Verlag: Berlin Heidelberg, Germany, 1984; pp 432–437.

Leslie, W. C. In *The Physical Metallurgy of Steels*; McGraw-Hill: New York, 1981; pp 68–108.

McKee, D. W. The Catalyzed Gasification Reactions of Carbon. In *Chemistry and Physics of Carbon*, Volume 16; Walker, P. L., Jr., Thrower, P. A., Eds.; Marcel Dekker, Inc.: New York, 1981; pp 1–118.

Newman, J. G.; Carlson, B. A.; Michael, R. S.; Molder, J. F. *Static SIMS Handbook of Polymer Analysis*; Hobilt, T. A., Ed.; Perkin-Elmer Corporation, Physical Electronics Division: Eden Prairie, MN, 1991.

Pumnea, R. W.; Stadnick, J. M., Jr. Characterizing Steel Surface Cleanliness Utilizing Statistical Methods for Data Analysis. In *Second International Symposium on Statistical Process Control and Sensors in the Steel Industry*; The Metallurgical Society of the Canadian Institute of Mining and Metallurgy: Montreal, Quebec, Canada, 1988; pp 92–124.

Schuetzle, D.; Carter, R. O., III; deVries, J. E.; Dickie, R. A.; Coduti, P. L. Application of Surface Spectroscopy in Studies of Interfacial Chemistry of Automotive Paint Systems., submitted for publication in *Prog. Org. Coat.*, 1994.

Solet, I. S. Conductometric Method for the Determination of Carbon on the Surface of Nickel Strip. *Anal. Chem.* **1966**, *38*, 504.

Wojtkowiak, J. J.; Bender, H. S. Interrelationship between Steel Surfaces, Phosphatabity, and Corrosion Resistance. *Anti-Corros.* **1979**, *26*, 9–13.

Wojtkowiak, J. J.; Bender, H. S. The Determination of Organic Contaminants on Cold Rolled Steel Surfaces. General Motors Research Publication 3333; General Motors Research Laboratories, Warren, MI, 1980, 1–16.


*Received for review* January 27, 1994
*Revised manuscript received* June 13, 1994
*Accepted* July 21, 1994[⊛]

[⊛] Abstract published in *Advance ACS Abstracts,* October 1, 1994.